BIOCHEMISTRY
including biophysical chemistry & molecular biology

Article

pubs.acs.org/biochemistry

Toward a Detailed Description of the Pathways of Allosteric Communication in the GroEL Chaperonin through Atomistic Simulation

Thomas J. Piggot,[†] Richard B. Sessions, and Steven G. Burston*

School of Biochemistry, University of Bristol, Medical Sciences Building, University Walk, Bristol BS8 1TD, U.K.

Supporting Information

ABSTRACT: GroEL, along with its coprotein GroES, is essential for ensuring the correct folding of unfolded or newly synthesized proteins in bacteria. GroEL is a complex, allosteric molecule, composed of two heptameric rings stacked back to back, that undergoes large structural changes during its reaction cycle. These structural changes are driven by the cooperative binding and subsequent hydrolysis of ATP, by GroEL. Despite numerous previous studies, the precise mechanisms of allosteric communication and the associated structural changes remain elusive. In this paper, we describe a series of all-atom, unbiased, molecular dynamics simulations over relatively long (50−100 ns) time scales of a single, isolated GroEL subunit and also a heptameric GroEL ring, in the presence and absence of ATP. Combined with results from a distance restraint-biased simulation of the single ring, the atomistic details of the earliest stages of ATP-driven structural changes within this complex molecule are illuminated. Our results are in broad agreement with previous modeling studies of isolated subunits and with a coarse-grained, forcing simulation of the single ring. These are the first reported all-atom simulations of the GroEL single-ring complex and provide a unique insight into the role of charged residues K80, K277, R284, R285, and E388 at the subunit interface in transmission of the allosteric signal. These simulations also demonstrate the feasibility of performing all-atom simulations of very large systems on sufficiently long time scales on typical high performance computing facilities to show the origins of the earliest events in biologically relevant processes.

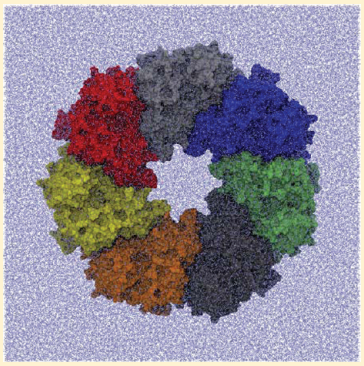

Allostery is an important method of regulating cellular processes by altering a protein's functional activity via changes in the conformation induced by the action of an effector. These effects can be exerted by changes in solvent conditions, covalent modifications, or the binding of another protein, or, more commonly, a small molecule substrate or ligand. Allosteric proteins can be thought to exist in a dynamic equilibrium of conformations that have different functional properties (e.g., weak and tight substrate binding), and the equilibrium between these conformations is shifted by the action of the effector that acts to stabilize one conformation over the others. In homotypic cooperativity, allosteric communication induced by the binding of a substrate initially causes local structural rearrangements as the free energy surface is perturbed, which in turn makes alternative conformations more accessible. A new energy minimum is reached as the intra- and intermolecular interactions rearrange in response to this perturbation (for reviews, see refs 1−3)

The GroEL chaperonin is an example of a highly complex allosteric system. It consists of two heptameric rings stacked back to back, with each subunit capable of binding and hydrolyzing ATP.[4] It functions with a coprotein, GroES, to assist the refolding of previously unfolded or newly synthesized proteins and is essential for bacterial cell viability.[5] Each subunit is composed of an equatorial domain that contains the ATP-binding site, the ring−ring contacts, and most of the intraring interactions and an apical domain that contains binding sites for the unfolded protein and GroES. These are linked by an intermediate domain containing two distinct hinge regions that provide a great deal of flexibility to each subunit (Figure 1A,B).

Each heptameric ring of GroEL binds ATP in a positively cooperative, concerted manner[6−8] that can be modeled using the MWC model of cooperativity.[9] The T state (apo) binds the polypeptide substrate tightly but ATP only weakly, while the R state has precisely the opposite properties.[10] Kinetically, after the rapid but weak binding of ATP to the T state, GroEL proceeds rapidly through three populated kinetic intermediates (R_{1-3}) until it reaches the stable holo conformation (R_4) (see the reaction scheme below).[11−14]

$$T \leftrightarrow R_1 \leftrightarrow R_2 \leftrightarrow R_3 \leftrightarrow R_4$$

Although there are no direct structural data about each of the kinetic intermediates arising between the T (apo) and R_4 conformations (which all arise on the 1−1000 ms time scale), mutations that affect this kinetic pathway at different stages and stabilize intermediate species have been identified.[15,16] In the functional cycle, this ATP-driven switch from the T conformation to the R_4 conformation is necessary to

Received: August 8, 2011
Revised: November 18, 2011
Published: January 30, 2012

dx.doi.org/10.1021/bi201237a | *Biochemistry* 2012, 51, 1707−1718

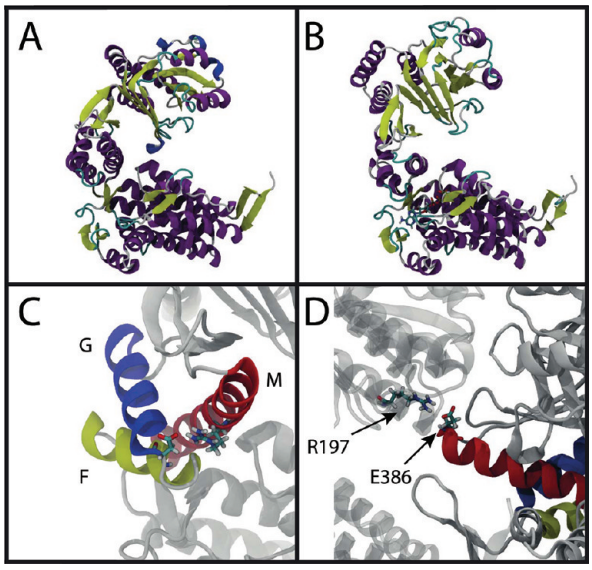

Figure 1. Structures of (A) an apo X-ray and (B) GroEL–ATP cryoEM subunits. Helices F (yellow), G (blue), and M (red) and the relevant Asp-155–Arg-395 (C) and Glu-386–Arg-197 (D) salt bridges of the intermediate domain.

ensure the binding of GroES and a concerted ejection of the bound polypeptide into the central cavity beneath GroES (i.e., the *cis* ring) where it is able to fold.[17] The effects of this transition from the T state to the R_4 state in one heptameric ring are also communicated across the ring–ring interface to the opposite ring, stabilizing the T conformation in that ring. Consequently, negative cooperativity is associated with the transition from the EL–$(ATP)_7$ form to the EL–$(ATP)_{14}$ form, which results in the affinity of the second ring for ATP being weaker than that of the first.[18,19] Once the seven ATP molecules in the *cis* ring have hydrolyzed to ADP, then this asymmetry between rings is exploited as the binding of ATP to the open (*trans*) ring is communicated back to the *cis* ring and induces the ejection of ADP, GroES, and the unfolded polypeptide substrate from that ring.[20−22] This means that allosteric communication within GroEL occurs over a long distance (65–70 Å) and is clearly an essential feature of the GroEL mechanism.

Although a complete understanding of the mechanism and pathway of allosteric communication in GroEL remains elusive, the end point structures have been determined. The structures of apo GroEL [Protein Data Bank (PDB) entry 1XCK][23] and the K-Mg-ATP-bound form (PDB entry 2C7E)[24] were determined by X-ray diffraction and cryo-electron microscopy (cryoEM), respectively, and define the T and R_4 states from the kinetic scheme. There are also crystallographic structures of two holo forms: a K-Mg-ATP-bound form (PDB entry 1KP8)[25] and a K-Mg-ATPγS-bound form (PDB entry 1SX3)[26] in which the subunit conformation is essentially the same as that observed in the apo model, presumably because crystal lattice packing forces have inhibited the ATP-induced structural changes. However, these latter structures reveal details about the atomic interactions among the protein, Mg^{2+}, K^+, and nucleotide. Analysis of the structural model built into the cryoEM reconstruction of the K-Mg-ATP-bound form reveals a 20° downward rotation of the intermediate domain that covers the nucleotide-binding site and brings the important catalytic residue Asp-398 into position for ATP hydrolysis, and an elevation of the apical domains accompanied by a 25° twisting in a counterclockwise direction[24] (Figure 1B). The X-ray structure of the GroEL–$(ADP)_7$–GroES complex reveals that further drastic conformational changes take place. This primarily involves a further opening of the apical domain by ~60° compared to the apo structure and a 110° clockwise rotation compared to the K-Mg-ATP cryoEM structure when viewed from above. However, because the simulations presented here were conducted in the absence of GroES, we primarily compare our results with the K-Mg-ATP cryoEM structure.

There has been a considerable amount of effort by various groups over the past decade to model these ATP-induced structural changes using a variety of computational approaches. The principal problem in modeling this process is the fact that the full conformational changes occur on the millisecond time scale and most allosteric systems, although not all, are fairly large, multisubunit complexes. This has previously made meaningful atomistic simulations impossible because of the massive amount of computer processing time needed. Consequently, simplifying approaches have generally been employed to overcome this limitation. The earliest such example examined the inherent low-frequency motions in a GroEL subunit, in the presence and absence of ATP, through normal-mode analysis and using a coarse-grained model in which each residue is represented by a Cα atom.[27] This and further computational studies, using the targeted molecular dynamics (TMD) method,[28] concluded that the initiating motion for the allosteric change was the downward movement of helix M in the intermediate domain toward the ATP-binding site that brings the important catalytic residue Asp-398 into the active site and also breaks the important Arg-197–Glu-386 salt bridge between subunits within a heptameric ring.[29] Experimentally, mutation of Arg-197 to alanine results in an almost complete loss of positive cooperativity within each heptameric ring,[30,31] supporting this finding. It was also suggested that the twisting and upward movement of the apical domain could be accommodated within the heptameric ring only if the movement is concerted, because of steric restrictions.[28]

Another early approach used CONCOORD simulations that generate different protein conformations based upon distance restraints derived from the interatomic interactions in the starting conformation,[32] and these are analyzed using covariance analysis. Simulations of the apo, ATPγS-bound (holo), and ADP–GroES-bound GroEL structures suggested that a displacement of the inter-ring contacts of Ala-108 and Ser-463 upon ATP binding may be important in the transmission of inter-ring allostery,[33] although there is no direct experimental evidence to support this.

Chaudhry et al.[26] made use of the information inherent in X-ray crystallographic data that provide information about the magnitude and direction of displacements of atoms from the observed structure using anisotropic displacement parameters. This translation–libration–screw (TLS) approach treats the domains as rigid bodies and uses the anisotropic displacement parameters to approximate the low-frequency motions in the system. Interestingly, this study revealed that inherent motions in the apo-GroEL structure were toward the folding active state (i.e., the GroES–ATP-bound structure), with a downward movement of the intermediate domain and an upward rotation of the apical domain, thus reflecting the dynamic conformational equilibrium between the apo and ATP-bound conformations even in the absence of ATP.

Another interesting informatics approach is the use of MAPS (Markov Propagation of Signals), which creates a network of all possible interactions and affinities between amino acids and then examines how perturbations in this network are communicated on a stochastic basis.[34] Using this approach, two pathways of allosteric communication were identified leading from the Ala-190−Lys-105 and the more important Arg-452−Glu-461 inter-ring contacts to the apical domains. Although there is experimental evidence supporting the important roles of Arg-452, Arg-97, and Glu-46, more experimental support for this information systems approach remains to be gathered.

More recently, long, coarse-grained simulations of the GroEL single subunit have been performed.[35,36] These simulations suggested that the initial trigger for the ATP-induced conformational transition was a downward tilt of two of the helices of the intermediate domain (F and M) followed by a switching salt bridge mechanism. This movement is then followed by a counterclockwise rotation of the apical domains toward the ATP-bound GroEL structure determined by cryoEM.[24] The second transition (R′ to R″ in their nomenclature) simulates the further structural rearrangements that take place in GroEL when GroES binds and ATP subsequently hydrolyzes. This transition is initiated by a further, rapid, decrease in the tilt of helices F and M upon ATP hydrolysis. The change in tilt is followed by a large clockwise rotation of the apical domain, especially of helices K and L, toward the R″ target structure and is accompanied by the formation of several salt bridges. This coarse-grained simulation is similar in some respects to the TMD method in that it requires prior knowledge of the end structures of the conformational change and is one of the major drawbacks of this method.

While the approaches mentioned above overcome the problem of insufficient computational power to model the system in an explicit all-atom manner, they also suffer some drawbacks. Either they attempt to determine the inherent routes of allosteric communication without explicit simulation of all the atoms within the GroEL molecule, or they involve a biasing introduced into the simulation to drive it toward a known structure without searching the conformational space along the transition path between structures. Recently, two 20 ns unbiased, all-atom molecular dynamics (MD) simulations of a single GroEL subunit in explicit solvent, and in the presence (holo) and absence (apo) of K-Mg-ATP, have been reported.[37] Abruptly, 6−8 ns after the launch of the simulation in the presence of K-Mg-ATP, a salt bridge in the intermediate domain (Asp-155−Arg-395) that anchors helices G and M in the intermediate domains was observed to break, followed by a rotation downward of helix M toward the ATP-binding pocket and a corresponding rotation of helices F and G (Figure 1C) in the same direction. The Asp-155−Arg-395 salt bridge is known to be important in the transmission of GroEL allostery because its removal resulted in the intraring cooperativity becoming sequential rather than concerted.[38] After alignment of the different structures from X-ray crystallography, cryoEM, and MD simulation, we concluded that although important salt bridges between subunits were broken and rearranged, there was little evidence of steric clashes enforcing the communication of allostery, in contradiction to previous work. The major drawback with these simulations is that because only one subunit is simulated, there are no intersubunit contacts, in particular no intersubunit Arg-197−Glu-386 salt bridge, to prevent the downward rotation of helix M.

In this paper, we present the results from a series of relatively long (50−100 ns) all-atom molecular dynamics simulations performed on a GroEL single subunit and GroEL single ring in explicit water with and without ATP. The structure of the GroEL single ring and the nature of the interface between single subunits of the ring are illustrated in Figure 2. We also present the results from novel distance restraint biasing (DRB) simulations that, when combined with the results from the unbiased simulations, provide insights into the atomistic detail of the mechanisms of allosteric communication within the context of the large, GroEL heptameric ring rather than the nonphysiological isolated subunit.

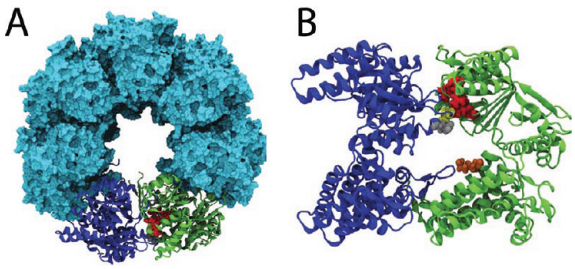

Figure 2. (A) GroEL single ring with two neighboring subunits highlighted in a cartoon representation and (B) interface between these two subunits with residues important in the intersubunit interactions highlighted in space filling representation. Glu-386 is colored yellow. Arg-197, Lys-277, Arg-284, and Arg-285 are colored red. Glu-388 is colored gray and Lys-80 orange.

MATERIALS AND METHODS

Simulation Setup. All simulations were performed within the GROMACS molecular dynamics package,[39] version 3.3.1,[40] using either the OPLS-AA/L[41] or AMBER-03[42,43] all-atom force field. ATP parameters used for both force fields were based upon those described in ref 44 and were validated for use with the OPLS-AA/L force field (for further details, see the Supporting Information). Coordinates for the starting models of GroEL were obtained from the Protein Data Bank entries 1XCK (apo-GroEL)[23] and 1SX3 (holo, K-Mg-ATP-bound).[26] The systems were constructed such that the protein was centered in a triclinic box with a minimal distance from the protein to the edge of the box of 2.0 nm. The box was filled with explicit water molecules, modeled using the TIP4P water model,[45] and the system was neutralized via random replacement of water molecules with sodium ions. Energy minimization was then performed using the steepest descent algorithm for 1000 steps. A short 200 ps position restraint simulation, in which the backbone of the protein was fixed in position using a force of 1000 kJ mol^{-1} nm^{-2}, was performed to allow an initial re-equilibration of the solvent molecules around the protein. After 200 ps, the position restraint forces were removed and the system was simulated for an additional "production" of 50 or 100 ns. Simulations were maintained at a constant temperature of 300 K and constant pressure of 1 bar using weak temperature and pressure coupling schemes.[46] Electrostatic interactions were calculated using a cutoff of 1.2 nm, with electrostatic interactions outside this cutoff treated using the particle mesh Ewald method.[47] Van der Waals interactions were truncated at 1.4 nm with a long-range

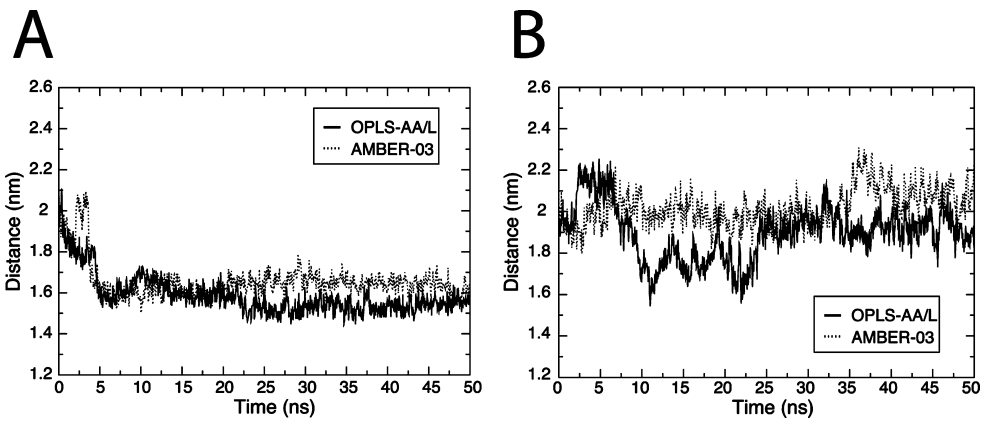

Figure 3. Distances between the center of mass (COM) of residue Thr-91 and the COM of the final turn of helix F, at the end closest to Thr-91, as it varies during (A) holo and (B) apo single-subunit simulations.

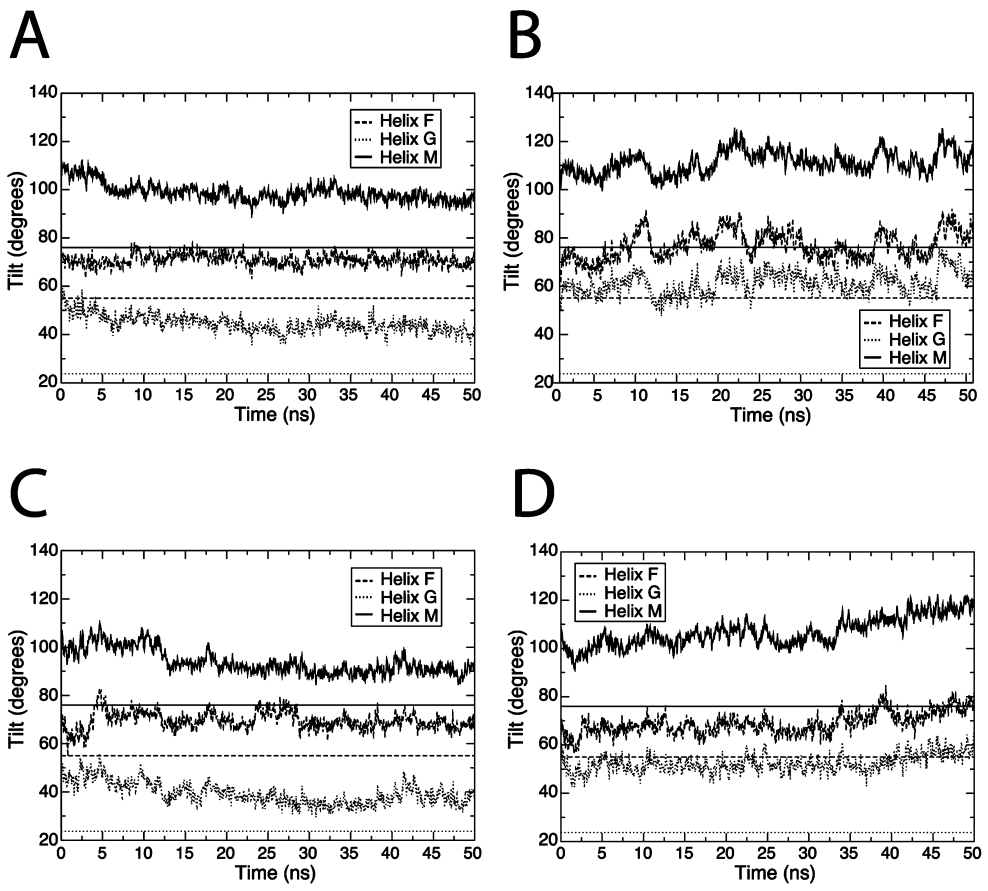

Figure 4. Changes in the orientation of helices F, G, and M of the intermediate domain calculated by the angle of the helix and the axis running vertically through the subunit for (A and C) holo and (B and D) apo single-subunit simulations. The orientations of these helices in the GroEL–$(ADP)_7$–GroES structure are shown as straight lines across each graph. A and B use the OPLS-AA/L forcefields. C and D use the AMBER-03 forcefield.

dispersion correction applied for energy and pressure. The neighbor list was updated every five steps during the simulations. All protein and ATP bonds during the simulations were constrained using the LINCS algorithm,[48] and water bonds and angles were constrained using the SETTLE algorithm.[49] These constraints allowed the use of a 2 fs time step. Coordinates were saved every 5 ps throughout the simulation for analysis with the tools provided by the GROMACS package[40] and for visual inspection with VMD.[50]

Distance Restraint Biasing (DRB) Simulations. These simulations were performed in the same manner as described for the normal MD simulations, until the stage of the production run. Instead of the unbiased molecular dynamics simulations, an additional biasing force intended to guide the simulation was applied, over a 10 ns length, in the direction of a target structure. The biasing force was generated through the following method. First, there was a random selection of 180 Cα atom pairs between the apical and equatorial domains within one subunit; 180 pairs were chosen so that all of the Cα

dx.doi.org/10.1021/bi201237a | *Biochemistry* 2012, 51, 1707–1718

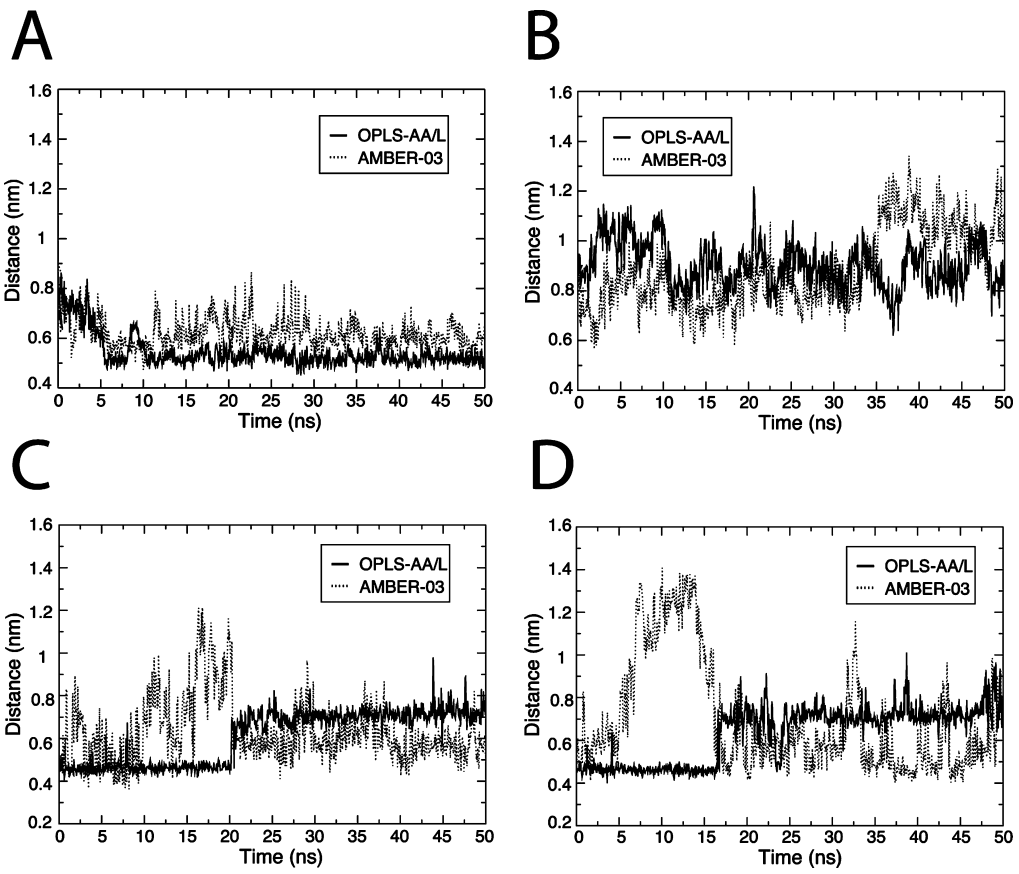

Figure 5. (A and B) Distances between the Cγ atom of the catalytic residue Asp-398 and the Cγ atom of Asp-87, the active site residue coordinated to the Mg^{2+} ion, in the (A) holo and (B) apo single-subunit simulations. (C and D) Distances between the Cγ atom of Asp-155 and the Cζ atom of Arg-395 for the (C) holo and (D) apo single-subunit simulations.

atoms in the apical domain were paired to a Cα atom in the equatorial domain. The distance among these 180 atom pairs was measured in both the starting and target structures, and the distance among these 180 atom pairs at the start of the simulation was restrained to be one-hundredth of the way toward the corresponding distances in the target structure. This was achieved by applying a harmonic restraint force of 222 kJ mol^{-1} nm^{-2} (or 10 kcal mol^{-1} $Å^{-2}$), and the simulation was performed for 100 ps. After this 100 ps, 180 new Cα atom pairs between the two domains were randomly chosen, and for the next 100 ps of the simulation, the distance among the 180 atom pairs was restrained at a distance two-hundredths of the way toward the corresponding distances in the target structure. This cycle continued for 100 steps until, for the last 100 ps of the 10 ns simulation, the restraint distance of the new random Cα atom pairs was equal to the distance in the target structure. This method is based upon that used by Chandra et al.,[51] who correctly predicted domain closure in the ternary complex of the glycolytic enzyme phosphoglycerate kinase, and it was this work that guided the choice of the force constant for the distance restraints.

Computer Hardware. Simulations were performed using the high-performance computing facility at the University of Bristol Advanced Computing Research Centre. Specifically, the Blue Crystal phase 2 facility consists of 416 nodes each with 2.8 GHz Intel Harpertown E5462 processors, 8 GB RAM per node, and 1 GB per core.

RESULTS

Single-Subunit Simulations. Simulations starting with either the apo single-subunit structure or the holo (ATP bound to the apo-like conformation) structure were performed for 50 ns using both the OPLS-AA/L or AMBER-03 force field. Overall, very similar dynamic behavior was observed with both force fields, while some specific differences are highlighted below. Much more significant was the difference in dynamic behavior between the apo and holo simulations. One of the major differences between simulations of the apo and holo subunits was observed in the conformational dynamics of the intermediate domain. In the holo simulations, there was a downward movement by ∼4.5 Å of helices F and G that occurred in the first 6−8 ns as monitored by the distance between Thr-91, the final residue of the γ-phosphate binding loop, and the closest end (defined as the center of mass of the final turn) of helix F (Figure 3A). This initial downward movement of helices F and G was accompanied by a progressive but much slower rotation of these helices by 10−15° toward the tilt observed in the GroEL−ATP and GroEL−ADP−GroES structures (Figure 4A,C). By contrast, the apo subunit shows no stable downward movement of helices F and G, although this conformation is sampled transiently during the simulation with the OPLS-AA/L force field (Figure 3B), and there was also no change in their tilt angle during the simulations (Figure 4B,D). It is known from the cryoEM GroEL−ATP structure and the GroEL−ADP−GroES X-ray structure that the ATP-induced downward movement of intermediate domain helix M brings the essential catalytic

dx.doi.org/10.1021/bi201237a | *Biochemistry* 2012, 51, 1707−1718

residue Asp-398 into position to activate a water molecule for the nucleophilic attack on the $\beta-\gamma$ phosphoanhydride bond. Therefore, the distance between the Cγ atom of Asp-398 and the Cγ atom of Asp-87, which coordinates the active site Mg^{2+} ion, was monitored throughout the simulation (Figure 5A,B). In the holo simulations, this distance decreased rapidly during the first 8 ns from ~8 to ~5 Å, while in the apo simulations, this distance fluctuated rapidly between ~7 and 12 Å. The salt bridge between Asp-155 on helix G and Arg-395 on helix M was also monitored. This electrostatic interaction anchors these two helices together in the apo conformation and has been hypothesized to exert a force on helix M that opposes the force that attracts Asp-398 toward the Mg^{2+} in the ATP-binding site.[37] In the simulations, this salt bridge is observed to break between 15 and 20 ns in both the apo and holo simulations using the OPLS-AA/L force field and does not re-form, while the same simulations using the AMBER-03 force field show the interaction to break quite early in the simulation and then re-form relatively stably after 15−20 ns (Figure 5C,D). To further highlight the differences in the movement of the intermediate domain between apo and holo simulations, the RMSD of the intermediate domain with respect to the intermediate domain conformation in the GroEL−ATP cryoEM structure was calculated after a superimposition of the equatorial domain from each frame onto the GroEL−ATP structure. These RMSDs (Figure 6), therefore, allow any movements of the intermediate domain toward the conformation in the GroEL−ATP structure to be quantified. In agreement with the previously measured distances and helical tilts, there are movements toward the GroEL−ATP cryoEM structure in both holo simulations; however, no such concerted movements exist in either apo simulation.

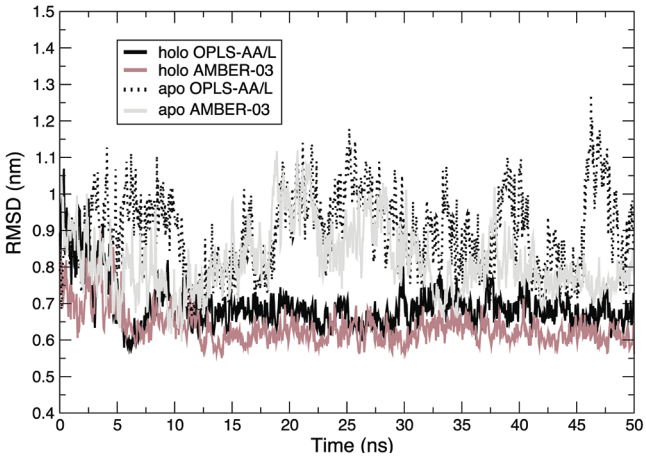

Figure 6. RMSDs of the intermediate domain during all four single-subunit simulations with respect to the GroEL−ATP cryoEM structure. The equatorial domain was used for the least-squares fitting.

The other major difference observed between apo and holo single-subunit simulations was in the dynamics of the apical domain. The RMSD of atoms within the apical domain was monitored and showed that this domain moves essentially as a rigid body throughout all of the single-subunit simulations (Figure S3 of the Supporting Information). However, a further RMSD calculation was performed in which the intermediate domain of every frame in the trajectory was superimposed onto the start structure and the RMSD for the apical domain relative to the intermediate domain was calculated (Figure 7A,B) to highlight the movement of the apical domain with respect to the intermediate domain. In the apo simulations, there was a substantial movement of the apical domain with respect to the intermediate domain, especially in the OPLS-AA/L simulation, showing the large amount of flexibility in the position of the apical domain in the apo subunit. In contrast, during both holo simulations, there was a reduced amount of movement of the apical domain throughout the 50 ns simulations.

Single-Ring Simulations. It is important to bear in mind that the previous simulations are of an isolated GroEL subunit, which is normally part of a complex of two heptameric rings stacked back to back. Therefore, the single-subunit simulations lack interactions with adjacent subunits that couple structural movements around the ring and may well provide resistance to some of the movements seen in the single-subunit simulations. To address this problem and to study the conformational dynamics of the subunits in a more realistic context, we performed simulations of both apo and holo GroEL single rings, again using both the OPLS-AA/L and AMBER-03 force fields. These systems comprised more than 520000 atoms and were performed for 50−100 ns.

In contrast to the single-subunit simulations, there was less movement within the subunits in all simulations, especially the movement of the apical domains. One major difference observed between apo and holo single-subunit simulations was the movement of the helices of the intermediate domain. Interestingly, this is also where the major difference was observed between the single-ring simulations. The distance between Thr-91 and the closest end of helix F was monitored as in the single-subunit simulations. In the apo simulations, this distance generally remained stable throughout the simulations (Figure 8B and Figure S4B of the Supporting Information), apart from some limited downward movement in two subunits during the apo AMBER-03 simulation. In contrast, during the holo OPLS-AA/L simulation, there was a downward movement of helices F and G by ~4.5−5 Å in four of the seven subunits (A, C, F, and G) (Figure 8A), which is similar to the movement observed in the single-subunit simulation (Figure 3A). In the AMBER-03 holo simulation, there was also a downward movement of five of the subunits in the ring, albeit to a lesser extent than in the OPLS-AA/L simulation (Figure S4A of the Supporting Information). However, in contrast to the single-subunit simulations, no substantial downward rotation of helix M was observed in any of the seven subunits in any apo or holo simulations, when the distance between Asp-398 and Asp-87 was monitored. In the OPLS-AA/L holo simulation, some transient downward rotations of helix M were observed in subunits A, C, F, and G; however, the extent of these never reached that seen in the GroEL−ATP cryoEM structure, and the atypical conformation quickly reverted back to the initial conformation (Figure 8C,D and Figure S4C,D of the Supporting Information).

The salt bridge between Glu-386 in one subunit and Arg-197 in the adjacent subunit has been shown to be a major interaction for the communication of intraring allostery[30,31] because it provides a direct link between movements in helix M and the neighboring subunit. Although this interaction has been well-characterized, inspection of the GroEL structure suggests that there are three other basic residues that may well be involved in forming intersubunit salt bridges with Glu-386, namely, Arg-284, Arg-285, and Lys-277. Therefore, the distance between Glu-386 and each of these basic residues in the

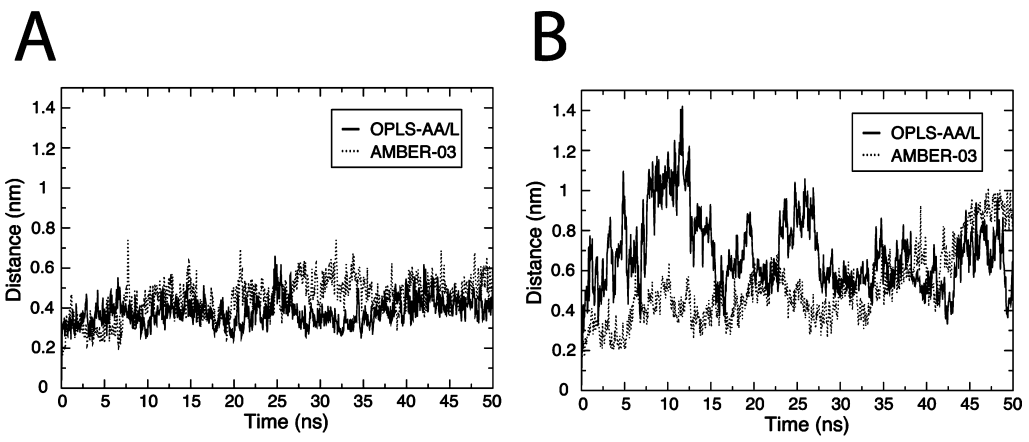

Figure 7. RMSDs of the apical domain with the intermediate domain used for the least-squares fitting of the (A) holo and (B) apo single-subunit simulations.

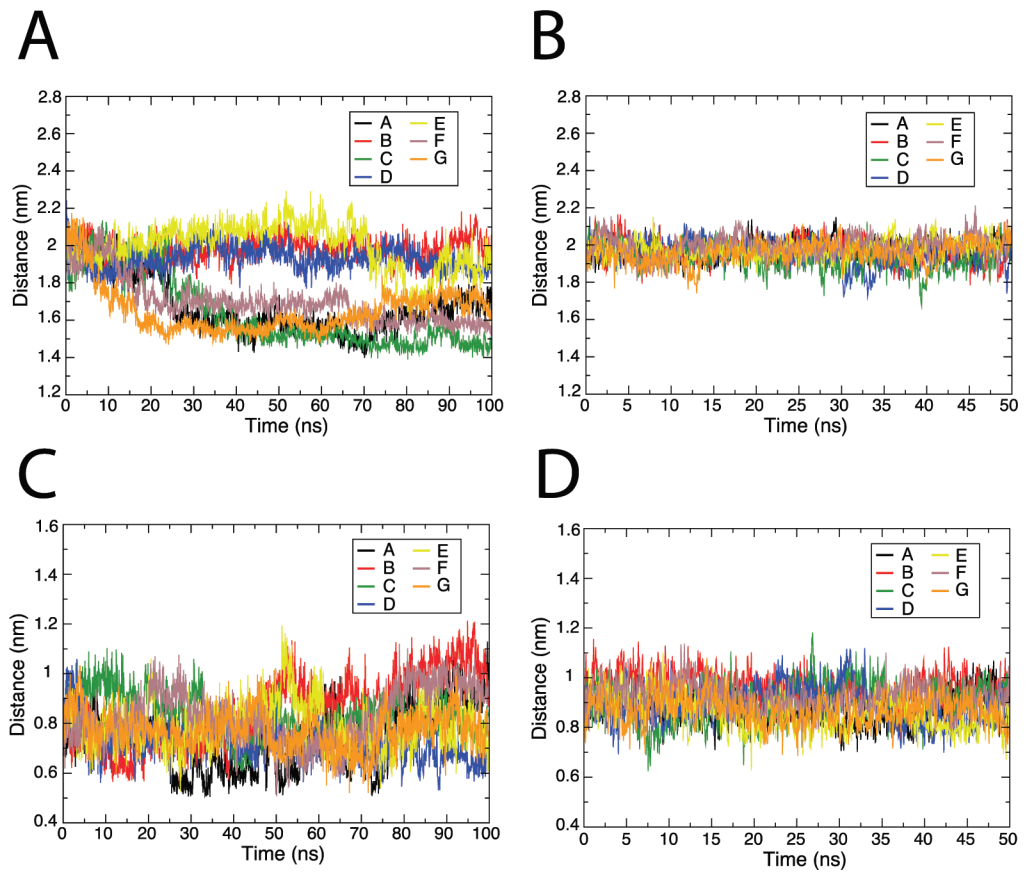

Figure 8. (A and B) Distances between the COM of Thr-91 and the COM of the final turn of helix F at the end located closest to Thr-91 as it varies for each subunit during the (A) holo and (B) apo GroEL OPLS-AA/L single-ring simulations. (C and D) Distances between the Cγ atom of catalytic residue Asp-398 and the Cγ atom of Asp-87, the active site residue coordinated to the Mg^{2+} ion, during the (C) holo and (D) apo OPLS-AA/L single-ring simulations.

adjacent subunit was monitored during the holo (Figures S5 and S6 of the Supporting Information) and apo (Figures S7 and S8 of the Supporting Information) simulations for all possible subunit pairs in the heptameric ring. The interactions formed between these pairs of residues during the single-ring simulations are summarized in Table 1. Although the Glu-386–Arg-197 interaction was reasonably stable in all the simulations, this salt bridge was observed to break at some points of the simulations (e.g., Figures S6E and S7D of the Supporting Information). However, at the same time that this salt bridge breaks, it was observed that Glu-386 formed an interaction with either Lys-277 or Arg-285 at any point in time, thus maintaining the intersubunit salt bridge interaction. Glu-386 seemed to interact only rarely with Arg-284, suggesting that Arg-284 is less important in the intersubunit interaction than Arg-197, Arg-285, or Lys-277.

Distance Restraint Biasing Simulations. DRB simulations were performed on the holo single ring in an attempt to

dx.doi.org/10.1021/bi201237a | *Biochemistry* 2012, 51, 1707–1718

Table 1. Intersubunit Salt Bridges Formed between Glu-386 and Arg-197, Lys-277, Arg-284, or Arg-285 during the Single-Ring Simulations[a]

	percentage of simulation time during which the salt bridges were formed			
Glu-386 interaction partner	holo OPLS-AA/L	holo AMBER-03	apo OPLS-AA/L	apo AMBER-03
Arg-197	76.6	29.1	61.6	23.0
Lys-277	43.5	21.5	61.2	57.3
Arg-284	0	0	8.3	0
Arg-285	16.0	39.6	27.7	58.0

[a]A salt bridge was counted as being formed if the distances between the COM of the side chain carboxylate group of Glu-386 and either the COM of the Cζ atom and both side chain NH_2 groups of Arg-197, Arg-284, or Arg-285 or the COM of the side chain amine group of Lys-277 were less than 0.4 nm. The percentages shown are averages over all seven subunit interfaces during the single-ring simulations.

force the simulations to overcome the interactions that stabilize the apo conformation within a reasonable simulation time scale. The RMSD of the individual subunits in the single ring with respect to the target structure during the DRB simulation (Figure S9 of the Supporting Information) show that the method is able to induce a conformational shift toward the target structure in all of the subunits. After 10 ns of DRB simulation, the salt bridges between Glu-386 and Arg-197, Arg-285, and Lys-277 are broken between all subunits, except between subunits F and G (see the initial values in Figure 9 and compare Figures 10A and 2B). It should be noted that during the DRB simulation the intermediate domain was not directly forced to change position but is responding to the induced movement of the apical domain of the neighboring subunit. After 10 ns of DRB simulation, the simulation was continued for a further 30 ns with the biasing forces removed. The distances between Glu-386 and Arg-197, Lys-277, and Arg-285 in the adjacent subunit were again monitored (Figure 9). During the 30 ns unbiased simulation, there was a re-formation of the Glu-386 salt bridges between all subunits except between subunits C and D and between subunits E and F. In the former case, Glu-388 of subunit C was able to form a new salt bridge to Lys-80 located in the equatorial domain of subunit D. The distance between Lys-80 of subunit D and both Glu-386 and Glu-388 of subunit C during the 30 ns unbiased simulation is shown in Figure 10B. The interface between subunits E and F showed a greater variation in the movement of helix M of subunit E. There was some movement upward toward the apical domain of subunit F and a transient interaction between Glu-386 and the 197/277/285 basic patch between 10 and 17 ns (Figure 9); however, helix M was then able to move downward toward the equatorial domain of subunit F.

DISCUSSION

This study compares relatively long, all-atom molecular dynamics simulations of a single, isolated subunit and a single heptameric ring of the GroEL chaperonin to analyze the origins of the ATP-induced allosteric changes that are central to the mechanism of this large protein complex. Although simulations of a GroEL subunit have been performed previously, we present here for the first time an all-atom simulation of a single, heptameric ring of GroEL, a large complex of 3745 amino acids in total.

Single-Subunit Simulations. The holo simulation was initiated from the ATP-bound structure (ATP bound to the apo conformation), and 6−8 ns into the simulation, there was a downward movement of helices F and G in the intermediate domain by ∼4.5 Å toward the position seen in the GroEL−ATP and GroEL−ADP−GroES structures. The corresponding downward movement of neighboring helix M brings the catalytic residue Asp-398 toward Asp-87 in the γ-phosphate binding loop. This movement of helices F and G has been observed in all other simulations using different theoretical approaches[26,28,35,37] and probably represents the earliest structural motions induced by the binding of ATP. At the same time, there was a much slower but progressive rotation of these two helices by 10−15° toward that seen in the GroEL−ATP cryoEM structure and the GroEL−ADP−GroES X-ray structure. The slow tilting of these helices compared to their rapid downward movement may be due to the fact that the apical domain has not proceeded through its opening and rotating motion observed in the GroEL−ATP cryoEM structure. In the apo simulations, no stable downward movement of helices F and G was observed and the distance between Asp-398 and Asp-87 oscillated by ±2.5 Å around the initial position. The salt bridge between Asp-155 in the equatorial domain and Arg-395 in the intermediate domain had been noted previously to be broken in simulations with ATP bound to GroEL but not in the apo simulations.[37] This might be expected because this bridge anchors helix M to G and therefore opposes the ATP-induced downward movement of helix M. However, in our simulations of the isolated subunit, this interaction was observed to break after 15−20 ns in the presence and absence of ATP. This break was not reversed when using the OPLS-AA/L force field, while simulations using the AMBER-03 force field showed the interaction breaking for ∼10 ns early in the simulation but then re-forming thereafter. In both simulations, there was very little movement within the apical domain, such that it could be considered to be moving as a rigid body. In the apo OPLS-AA/L simulation, it fluctuated quite markedly from its initial position, while in the holo simulations, the position of the domain with respect to the intermediate domain was relatively stable throughout the simulations regardless of whether the AMBER-03 or OPLS-AA/L force field was used. These differences may reflect a higher degree of coupling among the three domains in the holo structure, although because the subunit normally lies within a heptameric ring any movements would be dampened by interactions with adjacent subunits. The lack of either movement upward of the apical domains or changes in the orientation of the helices within the apical domain is in stark contrast to that seen in a previous unbiased molecular dynamics simulation of an isolated GroEL subunit with ATP bound[37] that reported a counterclockwise rotation of the apical domain by 15−30° and a deformation of the domain structure during this movement. It also contrasts with the result obtained by Ma et al.,[28] although their simulations used targeted molecular dynamics with an artificial force used to drive the conformational rearrangements toward a defined end point.

Single-Ring Simulations. Because binding of ATP to a GroEL heptameric ring is positively cooperative, simulations of the whole heptameric ring were performed to examine allosteric communication across the intersubunit interfaces within a ring. This approach is valid, despite the absence of the second heptameric ring, because an engineered single-ring version of GroEL (SR1) has been shown to mediate protein folding in

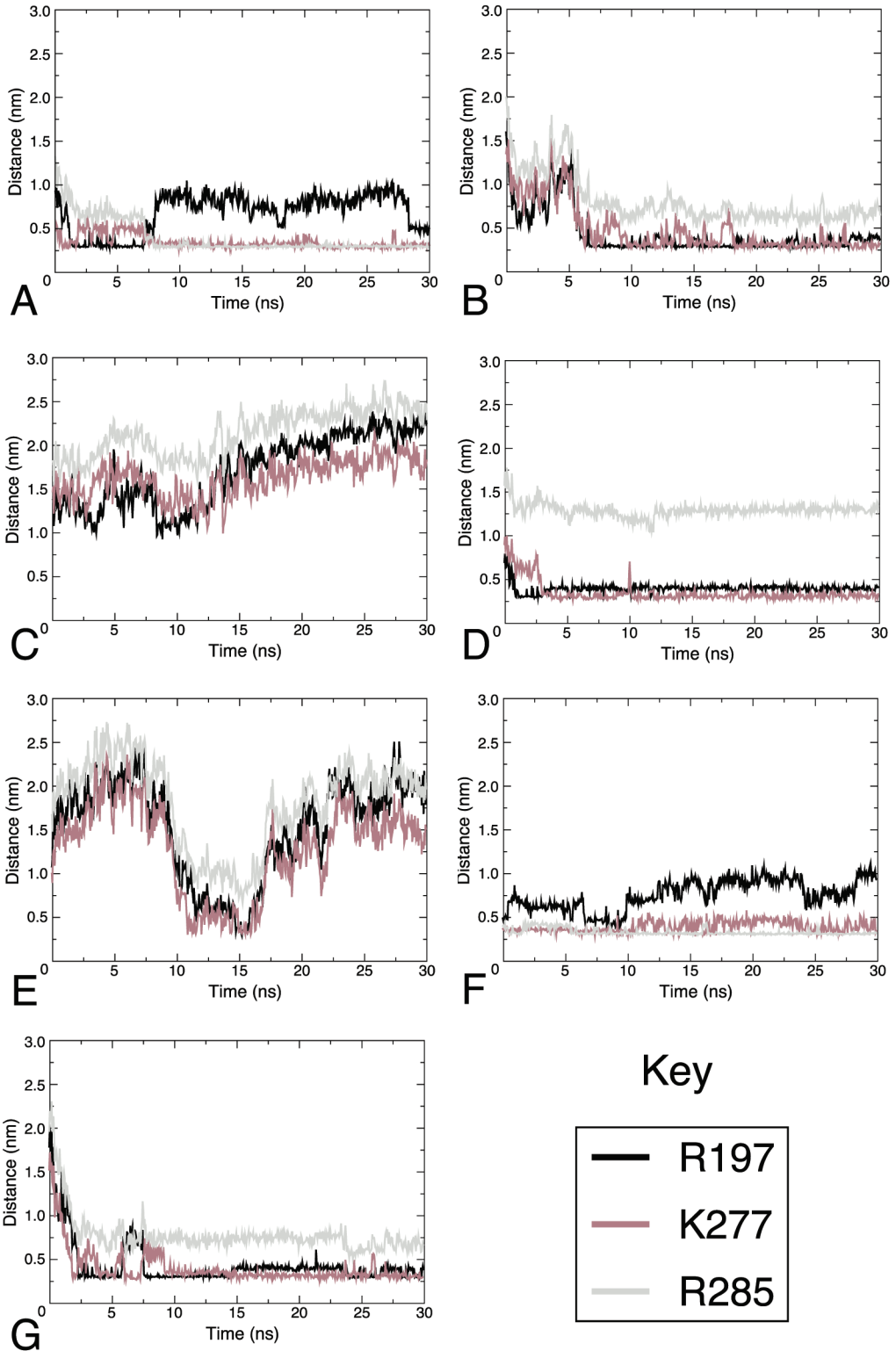

Figure 9. Distances between the COM of the side chain carboxylate group of Glu-386 and either the COM of the Cζ atom and both side chain NH_2 groups of Arg-197 or Arg-285 or the COM of the side chain amine group of Lys-277. The distance shown is between each pair of adjacent subunits in the 15 ns of unbiased simulation performed after 10 ns of biased simulation. Panel A shows the interaction of Glu-386 in subunit A with Arg-197, Arg-284, Arg-285, and Lys-277 in subunit B. Panel B shows the interactions of subunits B and C, etc.

vitro[52] and proceeds through similar structural changes upon ATP binding.[53,54] As expected, the presence of adjacent subunits had an overall effect of dampening any movement within subunits compared to the isolated subunit simulations. While the holo simulation gave rise to similar downward movements of helices F and G in four of the subunits within a ring (A, C, F, and G), there was no downward rotation of helix M. This contrasts with observations made in corresponding simulations of the isolated subunit. This is perhaps not surprising because an intersubunit salt bridge (Arg-197−Glu-

dx.doi.org/10.1021/bi201237a | *Biochemistry* 2012, 51, 1707−1718

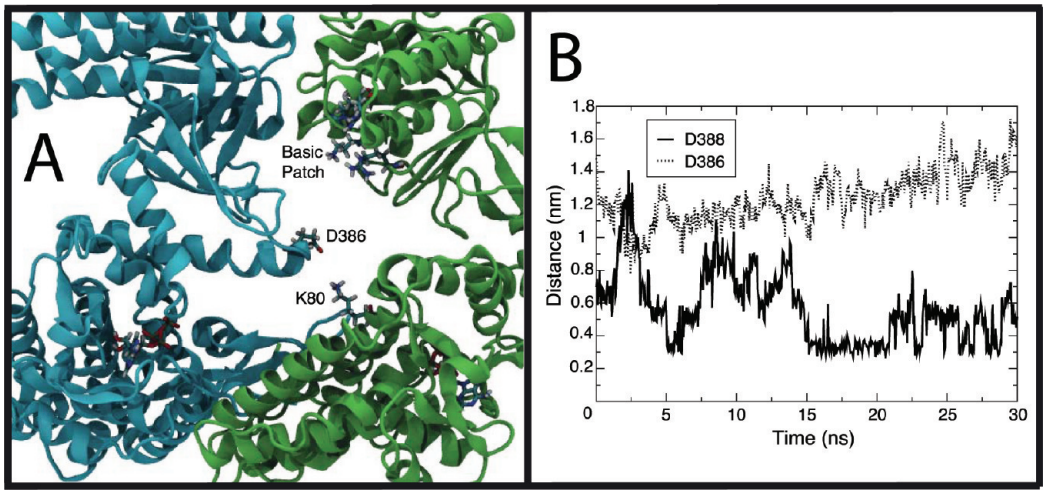

Figure 10. (A) Intersubunit interface showing the broken salt bridges between two of the subunits in the heptameric ring (subunits B and C) after 10 ns of DRB simulation. (B) Distances between the COM of the side chain amine group of Lys-80 in subunit D and the COM of the side chain carboxylate groups of Glu-386 or Glu-388 of subunit C during 30 ns of unbiased simulation.

386) that has been identified previously as being essential for intraring positive cooperativity[30] in ATP binding anchors in place the end of helix M that is distal to the ATP binding pocket, thus dampening this motion. However, the downward movement of helices F and G was observed in three adjacent subunits (A, F, and G, as well as C) over 25 ns, while a further subunit adjacent to this group (subunit E) began to show the same movement later in the simulation (after ~70 ns). It is tempting to speculate that this might be the beginning of intraring allosteric communication in that stochastic motions are stabilized in adjacent subunits to provide a conformational "seeding" that can then be spread throughout the remainder of the subunits.

The intersubunit interaction between Arg-197 and Glu-386 was reasonably stable in both the holo and apo simulations. Glu-386 was also observed to make reasonably stable interactions with Lys-277 and Arg-285 of the adjacent subunit. Arg-284 has been suggested previously to play a role in intersubunit interactions,[35] and Arg-285 has also been suggested to form a weak salt bridge with Glu-386.[31] However, Lys-277 has not (to the best of our knowledge) been identified as potentially having an important role in this intersubunit interaction with Glu-386, although mutation of this residue to glutamate was observed to decrease the steady state rate of the GroEL ATPase and was barely able to support growth of a GroEL-depleted strain of *E. coli*.[55] The interactions between Glu-386 and either Arg-285 or Lys-277, even when the Glu-386−Arg-197 salt bridge had been broken, anchored helix M to the adjacent subunit, ensuring that there was no downward rotation of this helix during these simulations. These interactions may serve to stabilize the apo conformation (T state) of GroEL by enhancing the coupling of subunits within a ring, thus providing a significant energy barrier in the transition to the R state that can be overcome only upon binding of ATP. Although this was not seen during these simulations, it must be borne in mind that the conformational transition normally takes place on the 10^{-3} to 1 s time scale while these simulations last for only 10^{-7} s.

Distance Restraint Biasing Simulations. DRB is similar to TMD in that a structure is driven between two conformations but is specifically designed to impose the least possible influence on the path taken to achieve the conformational transition.[51] During the simulations, the stabilizing salt bridges between Glu-386 and Arg-197, Arg-285, and Lys-277 were broken, thus allowing helix M to rotate downward bringing the catalytic Asp-398 into position for ATP hydrolysis. These simulations identified a new interaction between Glu-388 and Lys-80 in the equatorial domain. Lys-80 had been previously proposed to interact with Glu-386 during the ATP-induced structural rearrangements in GroEL.[35] Glu-388 was also identified in a random mutagenesis screen that identified point mutations in the single-ring version of GroEL (SR1) that allowed SR1 to render viability to a GroEL-depleted strain of *E. coli*.[56] These mutants affect GroES affinity, despite the fact that they are generally in the equatorial or intermediate domains, by affecting the pathways of allosteric communication.[16]

Concluding Remarks. The molecular dynamics simulations performed here on components of the GroEL chaperone comprise all-atom, explicit solvent, NPT ensembles simulated under periodic boundary conditions. We show that the underlying conformational transitions in a single subunit are largely independent of the particular force field used (AMBER-03 and OPLS-AA/L) and reproduce motions seen in previous studies. The beginnings of similar motions are observed during a 100 ns simulation of a heptameric ring of GroEL in which residues Lys-277, Arg-285, and Arg-284 help to stabilize the apo conformation of GroEL, thus dampening the structural fluctuations observed in simulations of the isolated subunit. Application of DRB to the heptameric ring complex revealed the role of these residues and the salt bridge between Lys-80 and Glu-388 in stabilizing structural intermediates during the allosteric transition. The making and breaking of this network of intersubunit salt bridges during the allosteric transmission of information is highly reminiscent of that observed in hemoglobin.[57] So far, our studies have focused on the ATP-induced motions in the single ring of GroEL; however, it will be interesting to determine how these structural dynamics are altered in the presence of the second GroEL ring, ADP, polypeptide substrate, and also the co-chaperonin GroES, as computing power is increased.

dx.doi.org/10.1021/bi201237a | *Biochemistry* 2012, 51, 1707−1718

■ ASSOCIATED CONTENT

Supporting Information

Detailed description of the validation of the ATP parameters for use with the OPLS-AA/L force field and a total of nine figures that further illustrate the work described in the paper. This material is available free of charge via the Internet at http://pubs.acs.org.

■ AUTHOR INFORMATION

Corresponding Author

*Telephone: +44 117 3312137. Fax: +44 117 3312168. E-mail: s.g.burston@bristol.ac.uk.

Present Address

†School of Chemistry, University of Southampton, University Road, Southampton SO17 1BJ, U.K.

Funding

We thank the BBSRC (UK) for a Strategic Award (BBSSH200511919), and provision of the high performance computing was from the University of Bristol via the Advanced Computing Research Centre (http://www.acrc.bris.ac.uk).

■ ABBREVIATIONS

COM, center of mass; DRB, distance restraint biasing; MAPS, Markov propagation of signals; MD, molecular dynamics; RMSD, root-mean-square deviation; TLS, translation−libration−screw; TMD, targeted molecular dynamics; cryoEM, cryo-electron microscopy.

■ REFERENCES

(1) Tsai, C. J., Del Sol, A., and Nussinov, R. (2009) Protein allostery, signal transmission and dynamics: A classification scheme of allosteric mechanisms. *Mol. Biosyst. 5*, 207−216.

(2) Cui, Q., and Karplus, M. (2008) Allostery and cooperativity revisited. *Protein Sci. 17*, 1295−1307.

(3) Goodey, N. M., and Benkovic, S. J. (2008) Allosteric regulation and catalysis emerge via a common route. *Nat Chem. Biol. 4*, 474−482.

(4) Braig, K., Otwinowski, Z., Hegde, R., Boisvert, D. C., Joachimiak, A., Horwich, A. L., and Sigler, P. B. (1994) The crystal structure of the bacterial chaperonin GroEL at 2.8 Å. *Nature 371*, 578−586.

(5) Ellis, R. J., and van der Vies, S. M. (1991) Molecular chaperones. *Annu. Rev. Biochem. 60*, 321−347.

(6) Gray, T. E., and Fersht, A. R. (1991) Cooperativity in ATP hydrolysis by GroEL is increased by GroES. *FEBS Lett. 292*, 254−258.

(7) Jackson, G. S., Staniforth, R. A., Halsall, D. J., Atkinson, T., Holbrook, J. J., Clarke, A. R., and Burston, S. G. (1993) Binding and hydrolysis of nucleotides in the chaperonin catalytic cycle: Implications for the mechanism of assisted protein folding. *Biochemistry 32*, 2554−2563.

(8) Todd, M. J., Viitanen, P. V., and Lorimer, G. H. (1993) Hydrolysis of adenosine 5′-triphosphate by *Escherichia coli* GroEL: Effects of GroES and potassium ion. *Biochemistry 32*, 8560−8567.

(9) Monod, J., Wyman, J., and Changeux, J. P. (1965) On the nature of allosteric transitions: A plausible model. *J. Mol. Biol. 12*, 88−118.

(10) Badcoe, I. G., Smith, C. J., Wood, S., Halsall, D. J., Holbrook, J. J., Lund, P., and Clarke, A. R. (1991) Binding of a chaperonin to the folding intermediates of lactate dehydrogenase. *Biochemistry 30*, 9195−9200.

(11) Yifrach, O., and Horovitz, A. (1998) Transient kinetic analysis of adenosine 5′-triphosphate binding-induced conformational changes in the allosteric chaperonin GroEL. *Biochemistry 37*, 7083−7088.

(12) Cliff, M. J., Kad, N. M., Hay, N., Lund, P. A., Webb, M. R., Burston, S. G., and Clarke, A. R. (1999) A kinetic analysis of the nucleotide-induced allosteric transitions of GroEL. *J. Mol. Biol. 293*, 667−684.

(13) Taniguchi, M., Yoshimi, T., Hongo, K., Mizobata, T., and Kawata, Y. (2004) Stopped-flow fluorescence analysis of the conformational changes in the GroEL apical domain: Relationships between movements in the apical domain and the quaternary structure of GroEL. *J. Biol. Chem. 279*, 16368−16376.

(14) Cliff, M. J., Limpkin, C., Cameron, A., Burston, S. G., and Clarke, A. R. (2006) Elucidation of steps in the capture of a protein substrate for efficient encapsulation by GroE. *J. Biol. Chem. 281*, 21266−21275.

(15) Koike-Takeshita, A., Shimamura, T., Yokoyama, K., Yoshida, M., and Taguchi, H. (2006) Leu309 plays a critical role in the encapsulation of substrate protein into the internal cavity of GroEL. *J. Biol. Chem. 281*, 962−967.

(16) Kovacs, E., Sun, Z., Liu, H., Scott, D. J., Karsisiotis, A. I., Clarke, A. R., Burston, S. G., and Lund, P. A. (2010) Characterisation of a GroEL single-ring mutant that supports growth of *Escherichia coli* and has GroES-dependent ATPase activity. *J. Mol. Biol. 396*, 1271−1283.

(17) Papo, N., Kipnis, Y., Haran, G., and Horovitz, A. (2008) Concerted release of substrate domains from GroEL by ATP is demonstrated with FRET. *J. Mol. Biol. 380*, 717−725.

(18) Yifrach, O., and Horovitz, A. (1995) Nested cooperativity in the ATPase activity of the oligomeric chaperonin GroEL. *Biochemistry 34*, 5303−5308.

(19) Burston, S. G., Ranson, N. A., and Clarke, A. R. (1995) The origins and consequences of asymmetry in the chaperonin reaction cycle. *J. Mol. Biol. 249*, 138−152.

(20) Weissman, J. S., Kashi, Y., Fenton, W. A., and Horwich, A. L. (1994) GroEL-mediated protein folding proceeds by multiple rounds of binding and release of nonnative forms. *Cell 78*, 693−702.

(21) Burston, S. G., Weissman, J. S., Farr, G. W., Fenton, W. A., and Horwich, A. L. (1996) Release of both native and non-native proteins from a cis-only GroEL ternary complex. *Nature 383*, 96−99.

(22) Rye, H. S., Burston, S. G., Fenton, W. A., Beechem, J. M., Xu, Z., Sigler, P. B., and Horwich, A. L. (1997) Distinct actions of cis and trans ATP within the double ring of the chaperonin GroEL. *Nature 388*, 792−798.

(23) Bartolucci, C., Lamba, D., Grazulis, S., Manakova, E., and Heumann, H. (2005) Crystal structure of wild-type chaperonin GroEL. *J. Mol. Biol. 354*, 940−951.

(24) Ranson, N. A., Farr, G. W., Roseman, A. M., Gowen, B., Fenton, W. A., Horwich, A. L., and Saibil, H. R. (2001) ATP-bound states of GroEL captured by cryo-electron microscopy. *Cell 107*, 869−879.

(25) Wang, J., and Boisvert, D. C. (2003) Structural basis for GroEL-assisted protein folding from the crystal structure of (GroEL-KMgATP)14 at 2.0 Å resolution. *J. Mol. Biol. 327*, 843−855.

(26) Chaudhry, C., Horwich, A. L., Brunger, A. T., and Adams, P. D. (2004) Exploring the structural dynamics of the *E. coli* chaperonin GroEL using translation-libration-screw crystallographic refinement of intermediate states. *J. Mol. Biol. 342*, 229−245.

(27) Ma, J., and Karplus, M. (1998) The allosteric mechanism of the chaperonin GroEL: A dynamic analysis. *Proc. Natl. Acad. Sci. U.S.A. 95*, 8502−8507.

(28) Ma, J., Sigler, P. B., Xu, Z., and Karplus, M. (2000) A dynamic model for the allosteric mechanism of GroEL. *J. Mol. Biol. 302*, 303−313.

(29) Xu, Z., Horwich, A. L., and Sigler, P. B. (1997) The crystal structure of the asymmetric GroEL-GroES-$(ADP)_7$ chaperonin complex. *Nature 388*, 741−750.

(30) Yifrach, O., and Horovitz, A. (1994) Two lines of allosteric communication in the oligomeric chaperonin GroEL are revealed by the single mutation Arg196→Ala. *J. Mol. Biol. 243*, 397−401.

(31) White, H. E., Chen, S., Roseman, A. M., Yifrach, O., Horovitz, A., and Saibil, H. R. (1997) Structural basis of allosteric changes in the GroEL mutant Arg197→Ala. *Nat. Struct. Biol. 4*, 690−694.

(32) de Groot, B. L., van Aalten, D. M., Scheek, R. M., Amadei, A., Vriend, G., and Berendsen, H. J. (1997) Prediction of protein conformational freedom from distance constraints. *Proteins 29*, 240−251.

(33) de Groot, B. L., Vriend, G., and Berendsen, H. J. (1999) Conformational changes in the chaperonin GroEL: New insights into the allosteric mechanism. *J. Mol. Biol. 286*, 1241−1249.
(34) Chennubhotla, C., and Bahar, I. (2006) Markov propagation of allosteric effects in biomolecular systems: Application to GroEL-GroES. *Mol. Syst. Biol. 2*, 36.
(35) Hyeon, C., Lorimer, G. H., and Thirumalai, D. (2006) Dynamics of allosteric transitions in GroEL. *Proc. Natl. Acad. Sci. U.S.A. 103*, 18939−18944.
(36) Stan, G., Lorimer, G. H., Thirumalai, D., and Brooks, B. R. (2007) Coupling between allosteric transitions in GroEL and assisted folding of a substrate protein. *Proc. Natl. Acad. Sci. U.S.A. 104*, 8803−8808.
(37) Sliozberg, Y., and Abrams, C. F. (2007) Spontaneous conformational changes in the *E. coli* GroEL subunit from all-atom molecular dynamics simulations. *Biophys. J. 93*, 1906−1916.
(38) Danziger, O., Rivenzon-Segal, D., Wolf, S. G., and Horovitz, A. (2003) Conversion of the allosteric transition of GroEL from concerted to sequential by the single mutation Asp-155 → Ala. *Proc. Natl. Acad. Sci. U.S.A. 100*, 13797−13802.
(39) Berendsen, H. J. C., van der Spoel, D., and van Drunen, R. (1995) GROMACS 3.0: A message-passing parallel molecular dynamics implementation. *Comput. Phys. Commun. 91*, 43−56.
(40) Lindahl, E., Hess, B., and van der Spoel, D. (2001) GROMACS 3.0: A package for molecular simulation and trajectory analysis. *J. Mol. Model. 7*, 306−317.
(41) Kaminski, G. A., Friesner, R. A., Tirado-Rives, J., and Jorgensen, W. L. (2001) Evaluation and reparameterization of the OPLS-AA force field for proteins via comparison with accurate quantum chemical calculations on peptides. *J. Phys. Chem. B 105*, 6474−6487.
(42) Duan, Y., Wu, C., Chowdhury, S., Lee, M. C., Xiong, G., Zhang, W., Yang, R., Cieplak, P., Luo, R., Lee, T., Caldwell, J., Wang, J., and Kollman, P. A. (2003) A point-charge force field for molecular simulations of proteins based on condensed-phase quantum mechanical calculations. *J. Comput. Chem. 24*, 1999−2012.
(43) Sorin, E. J., and Pande, V. S. (2005) Exploring the helix-coil transition via all-atom equilibrium ensemble simulations. *Biophys. J. 88*, 2472−2493.
(44) Meagher, K. L., Redman, L. T., and Carlson, H. A. (2003) Development of polyphosphate parameters for use with the AMBER force field. *J. Comput. Chem. 24*, 1016−1025.
(45) Jorgensen, W. L., Chandrasekhar, J., Madura, J. D., Impey, R. W., and Klein, M. L. (1983) Comparison of simple potential functions for simulating liquid water. *J. Chem. Phys. 79*, 926−935.
(46) Berendsen, H. J. C., Postma, J., van Gunsteren, W., Di Nola, A., and Haak, J. (1984) Molecular dynamics with coupling to an external bath. *J. Chem. Phys. 81*, 3684−3689.
(47) Essman, U., Perela, L., Berkowitz, M. L., Darden, T., Lee, H., and Pedersen, L. G. (1995) A smooth particle mesh Ewald method. *J. Chem. Phys. 103*, 8577−8592.
(48) Hess, B., Bekker, H., Berendsen, H. J. C., and Fraaije, J. G. E. M. (1997) LINCS: A linear constraint solver for molecular simulations. *J. Comput. Chem. 18*, 1463−1472.
(49) Miyamoto, S., and Kollman, P. A. (1992) SETTLE: An analytical version of the SHAKE and RATTLE algorithms for rigid water molecules. *J. Comput. Chem. 13*, 952−962.
(50) Humphrey, W., Dalke, A., and Schulten, K. (1996) VMD: Visual Molecular Dynamics. *J. Mol. Graphics 14*, 33−38.
(51) Chandra, N. R., Muirhead, H., Holbrook, J. J., Bernstein, B. E., Hol, W. G. J., and Sessions, R. B. (1998) A general method of domain closure is applied to phosphoglycerate kinase and the result compared with the crystal structure of a closed conformation of the enzyme. *Proteins 30*, 372−380.
(52) Weissman, J. S., Hohl, C. M., Kovalenko, O., Kashi, Y., Chen, S., Braig, K., Saibil, H. R., Fenton, W. A., and Horwich, A. L. (1995) Mechanism of GroEL action: Productive release of polypeptide from a sequestered position under GroES. *Cell 83*, 577−587.
(53) Amir, A., and Horovitz, A. (2004) Kinetic analysis of ATP-dependent inter-ring communication in GroEL. *J. Mol. Biol. 338*, 979−988.
(54) Poso, D., Clarke, A. R., and Burston, S. G. (2004) A kinetic analysis of the nucleotide-induced allosteric transitions in a single-ring mutant of GroEL. *J. Mol. Biol. 338*, 969−977.
(55) Fenton, W. A., Kashi, Y., Furtak, K., and Horwich, A. L. (1994) Residues in chaperonin GroEL required for polypeptide binding and release. *Nature 371*, 614−619.
(56) Sun, Z., Scott, D. J., and Lund, P. A. (2003) Isolation and characterisation of mutants of GroEL that are fully functional as single rings. *J. Mol. Biol. 332*, 715−728.
(57) Perutz, M. F. (1970) Stereochemistry of cooperative effects in haemoglobin: Haem-haem interaction and the problem of allostery. *Nature 228*, 979−988.